ELSEVIER

Coordination Chemistry Reviews
150 (1996) 265–292

COORDINATION CHEMISTRY REVIEWS

Appendices

Contents

SSDI 0010-8545(95)01265-6

Appendix I. NMR properties of nuclei

Isotope	Spin (I)	Natural abundance (%)	Relative sensitivity[a]	g_I	γ_I[b]	NMR frequency (MHz at 2.3488 T)	Q[c]
^{1}H	1/2	99.98	1.00	5.5856912	2.6751987×10^{8}	100.000	—
^{2}H	1	1.56×10^{-2}	9.65×10^{-3}	0.8574376	4.106593×10^{7}	15.351	2.875×10^{-3}
^{3}H	1/2	0	1.21	5.957921	2.853473×10^{8}	106.664	—
^{3}He	1/2	1.3×10^{-4}	0.442	−4.255248	-2.037999×10^{8}	76.181	—
^{6}Li	1	7.42	8.50×10^{-3}	0.8220467	3.937092×10^{7}	14.717	-6.44×10^{-4}
^{7}Li	3/2	92.58	0.294	2.170949	1.039750×10^{8}	38.866	-3.66×10^{-2}
^{9}Be	3/2	100	1.39×10^{-2}	−0.7852	-3.7606×10^{7}	14.057	5.3×10^{-2}
^{10}B	3	19.58	1.99×10^{-2}	0.600217	2.87466×10^{7}	10.746	8.472×10^{-3}
^{11}B	3/2	80.42	0.165	1.792425	8.58460×10^{7}	32.090	4.065×10^{-2}
^{13}C	1/2	1.108	1.59×10^{-2}	1.404822	6.72822×10^{7}	25.150	—
^{14}N	1	99.63	1.01×10^{-3}	0.4037607	1.933763×10^{7}	7.228	1.56×10^{-2}
^{15}N	1/2	0.37	1.04×10^{-3}	−0.5663784	-2.712600×10^{7}	10.140	—
^{17}O	5/2	3.7×10^{-2}	2.91×10^{-2}	−0.75752	-3.62803×10^{7}	13.562	-2.578×10^{-2}
^{19}F	1/2	100	0.834	5.257732	2.518127×10^{8}	94.129	—
^{21}Ne	3/2	0.257	2.46×10^{-3}	−0.441197	-2.11306×10^{7}	7.899	1.029×10^{-1}
^{23}Na	3/2	100	9.27×10^{-2}	1.478347	7.080361×10^{7}	26.467	1.01×10^{-1}
^{25}Mg	5/2	10.13	2.68×10^{-3}	−0.34218	-1.63883×10^{7}	6.126	0.22
^{27}Al	5/2	100	0.207	1.456602	6.976216×10^{7}	26.077	0.140
^{29}Si	1/2	4.7	7.86×10^{-3}	−1.11058	-5.3190×10^{7}	19.883	—
^{31}P	1/2	100	6.65×10^{-2}	2.26320	1.08393×10^{8}	40.518	—
^{33}S	3/2	0.76	2.27×10^{-3}	0.429214	2.05567×10^{7}	7.684	-6.4×10^{-2}
^{35}Cl	3/2	75.53	4.72×10^{-3}	0.5479157	2.624176×10^{7}	9.809	-8.249×10^{-2}
^{37}Cl	3/2	24.47	2.72×10^{-3}	0.4560820	2.184349×10^{7}	8.165	-6.493×10^{-2}
^{39}K	3/2	93.1	5.10×10^{-4}	0.2609772	1.249918×10^{7}	4.672	4.9×10^{-2}
^{41}K	3/2	6.88	8.43×10^{-5}	0.1432466	6.860621×10^{6}	2.565	6.0×10^{-2}
^{43}Ca	7/2	0.145	6.42×10^{-3}	−0.37636	-1.80253×10^{7}	6.738	—
^{45}Sc	7/2	100	0.302	1.358995	6.508741×10^{7}	24.330	−0.22
^{47}Ti	5/2	7.28	2.10×10^{-3}	−0.31539	-1.51053×10^{7}	5.646	0.29
^{49}Ti	7/2	5.51	3.78×10^{-3}	−0.31548	-1.51094×10^{7}	5.648	0.24
^{50}V	6	0.24	5.58×10^{-2}	0.557908	2.67203×10^{7}	9.988	7×10^{-2}

^{51}V	7/2	99.76	0.384	1.47183	7.0491×10^{7}	26.350	-5.2×10^{-2}
^{53}Cr	3/2	9.55	9.08×10^{-4}	−0.31636	-1.51517×10^{7}	5.664	2.2×10^{-2}
^{55}Mn	5/2	100.00	0.176	1.3813	6.6155×10^{7}	24.729	0.40
^{57}Fe	1/2	2.19	3.42×10^{-5}	0.1812459	8.680549×10^{6}	3.245	—
^{59}Co	7/2	100.00	0.278	1.322	6.332×10^{7}	23.67	0.404
^{61}Ni	3/2	1.19	3.59×10^{-3}	−0.50001	-2.39475×10^{7}	8.952	0.162
^{63}Cu	3/2	69.09	9.34×10^{-2}	1.4822	7.0988×10^{7}	26.536	−0.209
^{65}Cu	3/2	30.91	0.115	1.5878	7.6046×10^{7}	28.426	−0.195
^{67}Zn	5/2	4.11	2.87×10^{-3}	0.350191	1.677198×10^{7}	6.269	0.150
^{69}Ga	3/2	60.4	6.97×10^{-2}	1.34439	6.43881×10^{7}	24.069	0.168
^{71}Ga	3/2	39.60	0.143	1.70818	8.18112×10^{7}	30.581	0.106
^{73}Ge	9/2	7.76	1.41×10^{-3}	−0.1954371	-9.360221×10^{6}	3.499	−0.173
^{75}As	3/2	100.00	2.54×10^{-2}	0.95965	4.5961×10^{7}	17.180	0.29
^{77}Se	1/2	7.58	7.03×10^{-3}	1.07012	5.1252×10^{7}	19.158	—
^{79}Br	3/2	50.54	7.94×10^{-2}	1.404266	6.72556×10^{7}	25.140	0.293
^{81}Br	3/2	49.46	9.95×10^{-2}	1.513707	7.24971×10^{7}	27.100	0.27
^{83}Kr	9/2	11.55	1.90×10^{-3}	−0.215704	-1.033089×10^{7}	3.862	0.270
^{85}Rb	5/2	72.15	1.06×10^{-2}	0.54121	2.59207×10^{7}	9.689	0.274
^{87}Rb	3/2	27.85	0.177	1.83416	8.78449×10^{7}	32.837	0.132
^{87}Sr	9/2	7.02	2.71×10^{-3}	−0.242849	-1.16309×10^{7}	4.348	0.15
^{89}Y	1/2	100.00	1.19×10^{-4}	−0.2748306	-1.316268×10^{7}	4.920	—
^{91}Zr	5/2	11.23	9.49×10^{-3}	−0.52145	-2.49741×10^{7}	9.335	—
^{93}Nb	9/2	100.00	0.488	1.37122	6.5673×10^{7}	24.549	−0.36
^{95}Mo	5/2	15.72	3.27×10^{-3}	−0.3657	-1.7514×10^{7}	6.547	-1.9×10^{-2}
^{97}Mo	5/2	9.46	3.49×10^{-3}	−0.3734	-1.7884×10^{7}	6.785	−0.102
^{99}Ru	5/2	12.72	1.13×10^{-3}	−0.2565	-1.2286×10^{7}	4.592	7.6×10^{-2}
^{101}Ru	5/2	17.07	1.59×10^{-3}	−0.2875	-1.3770×10^{7}	5.147	0.44
^{103}Rh	1/2	100.00	3.17×10^{-5}	−0.17680	-8.468×10^{6}	3.165	—
^{105}Pd	5/2	22.23	1.13×10^{-3}	−0.2568	-1.230×10^{7}	4.60	0.8
^{107}Ag	1/2	51.82	6.72×10^{-5}	−0.227140	-1.08786×10^{7}	4.066	—

Appendix i. Continued.

Isotope	Spin (I)	Natural abundance (%)	Relative sensitivity[a]	g_I	γ_I[b]	NMR frequency (MHz at 2.3488 T)	Q[c]
^{109}Ag	1/2	48.18	1.02×10^{-4}	−0.2613810	-1.251852×10^{7}	4.679	—
^{111}Cd	1/2	12.75	9.66×10^{-3}	−1.1897712	-5.698264×10^{7}	21.300	—
^{113}Cd	1/2	12.26	1.11×10^{-2}	−1.2446010	-5.960865×10^{7}	22.282	—
^{113}In	9/2	4.28	0.351	1.22864	5.8844×10^{7}	21.996	0.846
^{115}In	9/2	95.72	0.353	1.23129	5.8971×10^{7}	2.044	0.861
^{115}Sn	1/2	0.35	3.56×10^{-2}	−1.83766	-8.8012×10^{7}	32.899	—
^{117}Sn	1/2	7.61	4.60×10^{-2}	−2.00208	-9.5887×10^{7}	35.843	—
^{119}Sn	1/2	8.58	5.27×10^{-2}	−2.09456	-1.00316×10^{8}	37.499	—
^{121}Sb	5/2	57.25	0.163	1.34536	6.4434×10^{7}	24.086	−0.20
^{123}Sb	7/2	42.75	4.66×10^{-2}	0.72851	3.4891×10^{7}	13.043	−0.26
^{123}Te	1/2	0.87	1.84×10^{-2}	−1.47358	-7.0575×10^{7}	26.381	—
^{125}Te	1/2	6.99	3.22×10^{-2}	−1.77656	-8.5086×10^{7}	31.806	—
^{127}I	5/2	100.00	9.54×10^{-2}	1.12531	5.38953×10^{7}	20.146	−0.789
^{129}Xe	1/2	26.44	2.16×10^{-2}	−1.55952	-7.45204×10^{7}	27.856	—
^{131}Xe	3/2	21.18	2.82×10^{-3}	0.461241	2.209056×10^{7}	8.258	−0.120
^{133}Cs	7/2	100.00	4.84×10^{-2}	0.7377209	3.533224×10^{7}	13.207	-3×10^{-3}
^{135}Ba	3/2	6.59	5.00×10^{-3}	0.558629	2.675484×10^{7}	10.001	0.18
^{137}Ba	3/2	11.32	7.00×10^{-3}	0.624910	2.992930×10^{7}	11.188	0.28
^{138}La	5	0.089	9.41×10^{-2}	0.74278	3.5575×10^{7}	13.298	0.51
^{139}La	7/2	99.911	6.06×10^{-2}	0.79520	3.8085×10^{7}	14.236	0.22
^{141}Pr	5/2	100.00	0.303	1.6544	7.924×10^{7}	29.62	-5.89×10^{-2}
^{143}Nd	7/2	12.17	3.39×10^{-3}	−0.3043	-1.457×10^{7}	5.45	−0.484
^{145}Nd	7/2	8.30	7.93×10^{-4}	−0.1874	-8.98×10^{6}	3.36	−0.253
^{147}Sm	7/2	14.97	1.52×10^{-3}	−0.23280	-1.1150×10^{7}	4.168	−0.18
^{149}Sm	7/2	13.83	8.52×10^{-4}	−0.19191	-9.192×10^{6}	3.436	5.2×10^{-2}
^{151}Eu	5/2	47.82	0.179	1.3887	6.6509×10^{7}	24.861	1.15
^{153}Eu	5/2	52.18	1.54×10^{-1}	0.6132	2.9368×10^{7}	10.978	2.94
^{155}Gd	3/2	14.73	1.48×10^{-3}	−0.1727	-8.273×10^{6}	3.092	1.59
^{157}Gd	3/2	15.68	3.34×10^{-4}	−0.2265	-1.0850×10^{7}	4.056	2.03
^{159}Tb	3/2	100.00	6.94×10^{-2}	1.343	6.431×10^{7}	24.04	1.18
^{161}Dy	5/2	18.88	4.75×10^{-4}	−0.1922	-9.205×10^{6}	3.441	2.44

^{163}Dy	5/2	24.97	1.30×10^{-3}	0.2690	1.2885×10^{7}	4.817	2.57
^{165}Ho	7/2	100.00	0.204	1.1923	5.710×10^{7}	21.35	2.73
^{167}Er	7/2	22.94	5.11×10^{-4}	−0.16186	-7.752×10^{6}	2.898	2.827
^{169}Tm	1/2	100.00	5.70×10^{-4}	−0.4632	-2.218×10^{7}	8.293	—
^{171}Yb	1/2	14.31	5.52×10^{-3}	0.98734	4.7287×10^{7}	17.676	—
^{173}Yb	5/2	16.13	1.35×10^{-3}	−0.271956	-1.30250×10^{7}	4.869	2.8
^{175}Lu	7/2	97.41	3.13×10^{-2}	0.63791	3.0552×10^{7}	11.421	5.68
^{176}Lu	7	2.59	4.05×10^{-2}	0.456	2.18×10^{7}	8.16	8
^{177}Hf	7/2	18.5	1.40×10^{-3}	0.22671	1.0858×10^{7}	4.059	4.5
^{179}Hf	9/2	13.75	5.47×10^{-4}	−0.14242	-6.821×10^{6}	2.550	5.1
^{181}Ta	7/2	99.99	3.74×10^{-2}	0.6771	3.243×10^{7}	12.12	3.9
^{183}W	1/2	14.40	7.50×10^{-5}	0.2355694	1.128231×10^{7}	4.217	—
^{185}Re	5/2	37.07	0.139	1.2748	6.1057×10^{7}	22.823	2.36
^{187}Re	5/2	62.93	0.143	1.2879	6.1681×10^{7}	23.057	2.24
^{187}Os	1/2	1.64	1.24×10^{-5}	0.12930	6.193×10^{6}	2.315	—
^{189}Os	3/2	16.10	2.44×10^{-3}	0.439955	2.107112×10^{7}	7.876	0.91
^{191}Ir	3/2	37.30	2.65×10^{-5}	0.0974	4.665×10^{6}	1.744	0.78
^{193}Ir	3/2	62.70	3.42×10^{-5}	0.1061	5.080×10^{6}	1.899	0.70
^{195}Pt	1/2	33.80	1.04×10^{-2}	1.21898	5.8382×10^{7}	21.823	—
^{197}Au	3/2	100.00	2.76×10^{-5}	0.098772	4.73056×10^{6}	1.768	0.594
^{199}Hg	1/2	16.84	5.94×10^{-3}	1.0117702	4.845750×10^{7}	18.114	—
^{201}Hg	3/2	13.22	1.49×10^{-3}	−0.373483	-1.788753×10^{7}	6.686	0.455
^{203}Tl	1/2	29.50	0.196	3.244514	1.553920×10^{8}	58.086	—
^{205}Tl	1/2	70.50	0.202	3.2764268	1.5692047×10^{8}	58.657	—
^{207}Pb	1/2	22.60	9.06×10^{-3}	1.16438	5.57666×10^{7}	20.846	—
^{209}Bi	9/2	100.00	0.144	0.91347	4.3749×10^{7}	16.354	−0.46
^{235}U	7/2	0.72	1.2×10^{-4}	−0.10	-4.3×10^{6}	1.8	4.55

[a] NMR sensitivity at constant field and equal number of nuclei, relative to ^{1}H nuclei, given by $4/3(|g_I|/|g_H|)^3 I(I+1)$.

[b] γ_I is defined by: $\gamma_I = g_I \mu_N/\hbar$, where the nuclear magneton, μ_N is 5.050824×10^{-27} J T^{-1}, and $\hbar$ is $1.0545877 \times 10^{-34}$ J s rad^{-1}.

[c] In units of 10^{-28} m^2.

Appendix II. Derivation of the equation for contact shift

The spin Hamiltonian for two contact coupled $S=\frac{1}{2}$, $I=\frac{1}{2}$ spins is given by

$$\mathcal{H} = g_e\mu_B B_0 S_z - \hbar\gamma_I B_0 I_z + A\boldsymbol{I}\cdot\boldsymbol{S}$$
$$= \tfrac{1}{2}Z_e - \tfrac{1}{2}Z_N + A[S_z I_z + \tfrac{1}{2}(S_+ I_- + S_- I_+)]$$

where Z_e and Z_N are the electron and nuclear Zeeman energies, and the energy matrix is

M_S, M_I	$\lvert\frac{1}{2},\frac{1}{2}\rangle$	$\lvert\frac{1}{2},-\frac{1}{2}\rangle$	$\lvert-\frac{1}{2},\frac{1}{2}\rangle$	$\lvert-\frac{1}{2},-\frac{1}{2}\rangle$
$\langle\frac{1}{2},\frac{1}{2}\rvert$	$\frac{1}{2}Z_e-\frac{1}{2}Z_N+\frac{1}{4}A$	0	0	0
$\langle\frac{1}{2},-\frac{1}{2}\rvert$	0	$\frac{1}{2}Z_e+\frac{1}{2}Z_N-\frac{1}{4}A$	$\frac{1}{2}A$	0
$\langle-\frac{1}{2},\frac{1}{2}\rvert$	0	$\frac{1}{2}A$	$-\frac{1}{2}Z_e-\frac{1}{2}Z_N-\frac{1}{4}A$	
$\langle-\frac{1}{2},-\frac{1}{2}\rvert$	0	0	0	$-\frac{1}{2}Z_e+\frac{1}{2}Z_N+\frac{1}{4}A$

Diagonalization of the above matrix yields the following energies and eigenfunctions:

$$E_1 = \tfrac{1}{2}Z_e - \tfrac{1}{2}Z_N + \tfrac{1}{4}A \qquad \Psi_1 = |\tfrac{1}{2},\tfrac{1}{2}\rangle$$
$$E_2 = -\tfrac{1}{4}A + \tfrac{1}{2}R \qquad \Psi_2 = c_1|\tfrac{1}{2},-\tfrac{1}{2}\rangle + c_2|-\tfrac{1}{2},\tfrac{1}{2}\rangle$$
$$E_3 = -\tfrac{1}{4}A - \tfrac{1}{2}R \qquad \Psi_3 = -c_2|\tfrac{1}{2},-\tfrac{1}{2}\rangle + c_1|-\tfrac{1}{2},\tfrac{1}{2}\rangle$$
$$E_4 = -\tfrac{1}{2}Z_e + \tfrac{1}{2}Z_N + \tfrac{1}{4}A \qquad \Psi_4 = |-\tfrac{1}{2},-\tfrac{1}{2}\rangle$$

where

$$R = (A^2 + (Z_e + Z_N)^2)^{1/2} \qquad c_1 = \left[\frac{1}{2}\left(1 + \frac{Z_e + Z_N}{R}\right)\right]^{1/2}$$

$$c_2 = \left[\frac{1}{2}\left(1 - \frac{Z_e + Z_N}{R}\right)\right]^{1/2}$$

Nuclear transition energies are given by $E_2 - E_1$ and $E_4 - E_3$. By referring for simplicity to the high field limit, i.e. when $Z_e \gg A$, we have

$$E_2 - E_1 = Z_N - \tfrac{1}{2}A \qquad E_4 - E_3 = Z_N + \tfrac{1}{2}A$$

The first transition is between states characterized by positive Z_e, the second between states with negative Z_e. Note that the nuclear transitions are separated by A and independent of S. However, the nucleus is only able to experience an average additional field from the magnetic moment of the electron, owing to its fast relaxation

between the two electronic states. The average transition energy is thus given by

$$\Delta E_{av} = P_+(Z_N - \tfrac{1}{2}A) + P_-(Z_N + \tfrac{1}{2}A) \tag{II.1}$$

where P_+ and P_- are the Boltzmann population of the electronic levels, as defined in Eq. (1.25). Eq. (II.1) can thus be rewritten as

$$\Delta E_{av} = \frac{\exp[-(Z_e/2kT)]}{\exp[-(Z_e/2kT)] + \exp(Z_e/2kT)}(Z_N - \tfrac{1}{2}A) + \frac{\exp(Z_e/2kT)}{\exp[-(Z_e/2kT)] + \exp(Z_e/2kT)}(Z_N + \tfrac{1}{2}A) \tag{II.2}$$

and, in the limit $Z_e \ll 2kT$:

$$\Delta E_{av} = \tfrac{1}{2}(1 - Z_e/2kT)(Z_N - \tfrac{1}{2}A) + \tfrac{1}{2}(1 + Z_e/2kT)(Z_N + \tfrac{1}{2}A)$$
$$= Z_N + \tfrac{1}{2}A\frac{Z_e}{2kT} = \hbar\gamma_I B_0 + A\frac{g_e\mu_B B_0}{4kT} \tag{II.3}$$

The contribution to the nuclear energy due to coupling with the unpaired electron, relative to the nuclear Zeeman energy equals the contact shift in ppm and is given by

$$\delta^{con} = A\frac{g_e\mu_B}{4\hbar\gamma_I kT} \tag{II.4}$$

which can be generalized for $S \neq \frac{1}{2}$ to obtain Eq. (2.5):

$$\delta^{con} = \frac{A}{\hbar}\frac{g_e\mu_B S(S+1)}{3\gamma_I kT} \tag{II.5}$$

Eq. (II.5) can also be obtained in a simpler way by recalling that for large magnetic fields the quantization axis of both the nuclear and the electron spins is along the external magnetic field. Therefore, the energy of the contact interaction from Hamiltonian (2.4) can be written as

$$E^{con} = AI_z\langle S_z\rangle = -AI_z\frac{g_e\mu_B S(S+1)B_0}{3kT} \tag{II.6}$$

where we have used the definition of $\langle S_z\rangle$ given in Eq. (1.31). The contact shift is again obtained by dividing the contact coupling energy by the nuclear Zeeman energy:

$$\delta^{con} = \frac{E_{con}}{\hbar\gamma_I I_z B_0} = \frac{A}{\hbar}\frac{g_e\mu_B S(S+1)}{3\gamma_I kT}$$

Appendix III. Derivation of the pseudocontact shift in the case of axial symmetry

We refer to the generic geometric arrangement of the electron and nuclear magnetic moments depicted in Fig. 2.6. The z axis of the cartesian coordinate frame, defined by the external magnetic field, is indicated by the unitary vector κ. The orientation of the molecular z axis is indicated by the unitary vector λ. The metal–nucleus vector is indicated by r. The angle between κ and λ is called α, the angle between λ and r is called θ, and the angle between κ and r is called γ. We also define a direction ν perpendicular to λ and lying in the $\kappa\lambda$ plane, and a direction ι perpendicular to the $\kappa\lambda$ plane. When performing rotational averaging, we will be dealing with rotations of the molecule about its principal axis λ; upon such rotation, the vector r will define a cone around λ, and it will be useful to define an angle Ω to locate r along the surface of the cone. Ω is zero when r lies in the $\kappa\lambda$ plane.

Our aim is that of evaluating the energy of the dipolar interaction between the nuclear and electron magnetic moments from the classical expression (see Eq. (1.1)):

$$E^{\mathrm{dip}} = -\left(\frac{\mu_0}{4\pi}\right)\frac{1}{r^3}\left[3\frac{(\langle\mu\rangle\cdot r)(\mu_{I\kappa}\cdot r)}{r^2} - \langle\mu\rangle\cdot\mu_{I\kappa}\right] \tag{III.1}$$

where $\langle\mu\rangle$ is the average induced magnetic moment of the electron, and $\mu_{I\kappa}$ is the projection of the nuclear magnetic moment along B_0. By referring to Fig. 2.6, $\mu_{I\kappa} = \hbar\gamma_I I_z\kappa$. From Eq. (1.27), we can write

$$\langle\mu\rangle = \frac{\chi_M}{N_A}\frac{B_0}{\mu_0} = \chi\frac{B_0}{\mu_0} \tag{III.2}$$

where χ is defined as the molecular magnetic susceptibility. We also know that χ is a tensorial quantity (cf. Eq. (1.40)). By analogy, the vector $\langle\mu\rangle$ can be obtained by taking the vector projection of the χ tensor along κ and rewriting Eq. (III.2) as

$$\langle\mu\rangle = \frac{B_0}{\mu_0}\chi\cdot\kappa \tag{III.3}$$

By recalling that $\lambda\cdot\kappa = \cos\alpha$, $\nu\cdot\kappa = -\sin\alpha$, and $\iota\cdot\kappa = 0$, we obtain

$$\langle\mu\rangle = \frac{B_0}{\mu_0}(\chi_\parallel\cos\alpha\lambda - \chi_\perp\sin\alpha\nu) \tag{III.4}$$

Note that $\langle\mu\rangle$ is slightly misaligned with respect to the direction of B_0, κ; it would be coincident with the κ direction only if $\chi_\parallel = \chi_\perp$, i.e. in the absence of magnetic susceptibility anisotropy.

By substituting Eq. (III.4) in Eq. (III.1), and recalling also that

$$\lambda\cdot r = r\cos\theta \qquad \nu\cdot r = -r\sin\theta\cos\Omega$$

$$\kappa\cdot r = r\cos\gamma = r(\cos\alpha\cos\theta + \sin\alpha\sin\theta\cos\Omega)$$

we obtain

$$E^{dip} = -\frac{B_0}{4\pi r^3}\hbar\gamma_I I_z[3(\chi_\parallel \cos\alpha\cos\theta + \chi_\perp \sin\alpha\sin\theta\cos\Omega)(\cos\alpha\cos\theta + \sin\alpha\sin\theta\cos\Omega) - (\chi_\parallel\cos^2\alpha + \chi_\perp\sin^2\alpha)] \quad \text{(III.5)}$$

which can be rearranged as

$$E^{dip} = -\frac{B_0}{4\pi r^3}\hbar\gamma_I I_z[\chi_\parallel\cos^2\alpha(3\cos^2\theta - 1) + \chi_\perp\sin^2\alpha(3\sin^2\theta\cos^2\Omega - 1) + \tfrac{3}{4}(\chi_\parallel + \chi_\perp)\sin 2\alpha\sin 2\theta\cos\Omega] \quad \text{(III.6)}$$

Eq. (III.6) is the general formula for the dipolar interaction energy when the principal axis of χ is in a generic λ direction. The shift is then obtained by calculating the energy difference between two states differing by $\Delta M_I = \pm 1$:

$$\Delta E^{dip} = -\frac{B_0}{4\pi r^3}\hbar\gamma_I[\chi_\parallel\cos^2\alpha(3\cos^2\theta - 1) + \chi_\perp\sin^2\alpha(3\sin^2\theta\cos^2\Omega - 1) + \tfrac{3}{4}(\chi_\parallel + \chi_\perp)\sin 2\alpha\sin 2\theta\cos\Omega] \quad \text{(III.7)}$$

and by dividing the result by the nuclear Zeeman energy $\hbar\gamma_I B_0$

$$\frac{\Delta E^{dip}}{\hbar\gamma_I B_0} = \delta^{dip} = \frac{1}{4\pi r^3}[\chi_\parallel\cos^2\alpha(3\cos^2\theta - 1) + \chi_\perp\sin^2\alpha(3\sin^2\theta\cos^2\Omega - 1) + \tfrac{3}{4}(\chi_\parallel + \chi_\perp)\sin 2\alpha\sin 2\theta\cos\Omega] \quad \text{(III.8)}$$

Eq. (III.8) gives the dipolar shift in the solid state (see Chapter 8). Note that when χ is isotropic it reduces to

$$\delta^{dip} = \frac{1}{4\pi r^3}\chi[3(\cos\alpha\cos\theta + \sin\alpha\sin\theta\cos\Omega)^2 - 1] = \frac{1}{4\pi r^3}\chi(3\cos^2\gamma - 1) \quad \text{(III.9)}$$

which gives the dipolar shift in magnetically isotropic solids and which averages zero in solution (cf. Eq. (2.15)).

To derive the pseudocontact shift in solution δ^{pc} we must now take the rotational average of Eq. (III.8). By recalling that

$$\frac{1}{2\pi}\int_0^{2\pi}\cos\Omega\,d\Omega = 0 \qquad \frac{1}{2\pi}\int_0^{2\pi}\cos^2\Omega\,d\Omega = \tfrac{1}{2}$$

integration of Eq. (III.8) in $d\Omega$ gives

$$\delta = \frac{1}{4\pi r^3}[\chi_\parallel\cos^2\alpha(3\cos^2\theta - 1) + \chi_\perp\sin^2\alpha(\tfrac{3}{2}\sin^2\theta - 1)] \quad \text{(III.10)}$$

We then need integrating over the solid angle α ($d\cos\alpha = \sin\alpha\, d\alpha$), and recalling that

$$\frac{1}{2}\int_0^{\pi} \cos^2\alpha \sin\alpha\, d\alpha = \frac{1}{3} \qquad \frac{1}{2}\int_0^{\pi} (1-\cos^2\alpha)\sin\alpha\, d\alpha = \frac{2}{3}$$

we obtain

$$\delta^{dip} = \frac{1}{4\pi r^3}\left[\chi_{\parallel}\tfrac{1}{3}(3\cos^2\theta - 1) + \chi_{\perp}\tfrac{1}{3}(3 - 3\cos^2\theta - 2)\right]$$

$$= \frac{1}{12\pi r^3}(\chi_{\parallel} - \chi_{\perp})(3\cos^2\theta - 1) \qquad \text{(III.11)}$$

which is Eq. (2.14).

Appendix IV. Derivation of the equations related to NOE

A necessary step to derive Eq. (6.2) and other equations in Chapter 6 is the obtaining of a suitable expression for the time dependence of M_z^I in a dipole-coupled two spin system. By referring to Fig 6.1, M_z^I and M_z^J are given by

$$M_z^I = K(P_{++} + P_{+-} - P_{-+} - P_{--}) \qquad M_z^J = K(P_{++} + P_{-+} - P_{+-} - P_{--}) \tag{IV.1}$$

The rate of variation of M_z^I with time, $dM_z^I(t)/dt$, is proportional to the rate of population increase of levels $++$ and $+-$ minus the rate of population increase of levels $-+$ and $--$:

$$\frac{dM_z^I(t)}{dt} = K\left(\frac{dP_{++}}{dt} + \frac{dP_{+-}}{dt} - \frac{dP_{-+}}{dt} - \frac{dP_{--}}{dt}\right) \tag{IV.2}$$

Among the various transitions shown in Fig. 6.1, we can neglect those involving only changes in spin state of J. For instance, the first of the four terms in the right-hand side of Eq. (IV.2) is:

$$\frac{dP_{++}}{dt} = -(w_1^I + w_2)P_{++} + w_1^I P_{-+} + w_2 P_{--} + c \tag{IV.3}$$

The constant c can be evaluated by setting $dP_{++}/dt = 0$:

$$c = (w_1^I + w_2)P_{++}(\infty) - w_1^I P_{-+}(\infty) - w_2 P_{--}(\infty) \tag{IV.4}$$

and Eq. (IV.3) becomes

$$\frac{dP_{++}}{dt} = -(w_1^I + w_2)\Delta P_{++} + w_1^I \Delta P_{-+} + w_2 \Delta P_{--} \tag{IV.5}$$

where

$$P - P(\infty) = \Delta P \tag{IV.6}$$

Analogous equations can be written for the other three terms in Eq. (IV.2). By grouping all the terms together, Eq. (IV.2) becomes

$$\begin{aligned}\frac{dM_z^I(t)}{dt} = K[&-2\Delta P_{++}(w_1^I + w_2) \\ &- 2\Delta P_{+-}(w_1^I + w_0) + 2\Delta P_{-+}(w_1^I + w_0) + 2\Delta P_{--}(w_1^I + w_2)]\end{aligned} \tag{IV.7}$$

which can be rearranged to

$$\frac{dM_z^I(t)}{dt} = 2K[(\Delta P_{--} - \Delta P_{++})(w_1^I + w_2) + (\Delta P_{-+} - \Delta P_{+-})(w_1^I + w_0)] \tag{IV.8}$$

The factor 2 derives from the fact that a single transition decreases the population of the starting state and at the same time increases the population of the target state, thereby changing the population difference by twice as much.

However, from Eq. (IV.1) we can write

$$M_z^I + M_z^J = -2K(P_{--} - P_{++}) \qquad M_z^I - M_z^J = -2K(P_{-+} - P_{+-}) \tag{IV.9}$$

and, using Eq. (IV.6)

$$\begin{aligned} M_z^I(t) - M_z^I(\infty) + M_z^J(t) - M_z^J(\infty) &= -2K(\Delta P_{--} - \Delta P_{++}) \\ M_z^I(t) - M_z^I(\infty) - M_z^J(t) + M_z^J(\infty) &= -2K(\Delta P_{-+} - \Delta P_{+-}) \end{aligned} \tag{IV.10}$$

Substituting Eq. (IV.10) into Eq. (IV.8) gives

$$\begin{aligned} \frac{dM_z^I(t)}{dt} = &-[M_z^I(t) - M_z^I(\infty) + M_z^J(t) - M_z^J(\infty)](w_1^I + w_2) \\ &- [M_z^I(t) - M_z^I(\infty) - M_z^J(t) + M_z^J(\infty)](w_1^I + w_0) \end{aligned} \tag{IV.11}$$

that finally becomes

$$\frac{dM_z^I(t)}{dt} = -[M_z^I(t) - M_z^I(\infty)](w_0 + 2w_1^I + w_2) - [M_z^J(t) - M_z^J(\infty)](w_2 - w_0) \tag{IV.12}$$

Eq. (IV.12) is the starting point to derive not only the equations relevant for the NOE phenomenon (Chapter 6) but also Eq. (3.12) and the following ones (Section 3.4). A somewhat different form of Eq. (IV.12) has already been encountered when dealing with transfer of magnetization between two sites in chemical exchange (Section 4.3.4).

According to the definitions given in Eqs. (6.3) and (6.4), Eq. (IV.12) can be rewritten as

$$\frac{dM_z^I(t)}{dt} = -[M_z^I(t) - M_z^I(\infty)]\rho_{I(J)} - [M_z^J(t) - M_z^J(\infty)]\sigma_{I(J)} \tag{IV.13}$$

Eq. (6.2), relevant for steady state NOE, can easily be obtained from Eq. (IV.13) by setting $dM_z^I(t)/dt = 0$ and $M_z^J(t) = 0$:

$$0 = -[M_z^I(t) - M_z^I(\infty)]\rho_{I(J)} + M_z^J(\infty)\sigma_{I(J)} \tag{IV.14}$$

which rearranges to

$$M_z^I(t) = M_z^I(\infty) + [\sigma_{I(J)}/\rho_{I(J)}]M_z^J(\infty) \tag{6.2}$$

For the homonuclear case, generalized by substituting $\rho_{I(J)}$ with the total relaxation rate ρ_I in Eq. (IV.13) and the following, we obtain

$$\frac{M_z^I(t) - M_z^I(\infty)}{M_z^I(\infty)} \tag{6.10}$$

The equation for truncated NOE (Section 6.3) can also be derived from Eq. (IV.13), again generalized by substituting $\rho_{I(J)}$ with the total relaxation rate ρ_I, by setting

$M_z^J(t) = 0$ (instantaneous saturation). Integration then gives

$$M_z^I(t) = A\exp(-\rho_I t) + B \tag{IV.15}$$

To evaluate the constants A and B we start by deriving again Eq. (15):

$$\frac{dM_z^I(t)}{dt} = -A\rho_I \exp(-\rho_I t) \tag{IV.16}$$

From Eq. (IV.15) we can then write

$$A\exp(-\rho_I t) = M_z^I(t) - B \tag{IV.17}$$

and, by substituting Eq. (IV.17) into Eq. (IV.16), we obtain

$$\frac{dM_z^I(t)}{dt} = -\rho_I M_z^I(t) + \rho_I B \tag{IV.18}$$

However, from Eq. (IV.13) under instantaneous saturation of J we can write

$$\frac{dM_z^I(t)}{dt} = -[M_z^I(t) - M_z^I(\infty)]\rho_I + M_z^J(\infty)\sigma_{I(J)} \tag{IV.19}$$

and, by equating the right-hand sides of Eqs. (IV.18) and (IV.19)

$$B = M_z^I(\infty) + [\sigma_{I(J)}/\rho_I]M_z^J(\infty) \tag{IV.20}$$

By substituting Eq. (IV.20) back into Eq. (IV.15) we obtain

$$M_z^I(t) = A\exp(-\rho_I t) + M_z^I(\infty) + [\sigma_{I(J)}/\rho_I]M_z^J(\infty) \tag{IV.21}$$

at $t = 0$, $M_z^I(t) = M_z^I(\infty)$, and therefore

$$A = -[\sigma_{I(J)}/\rho_I]M_z^J(\infty) \tag{IV.22}$$

from which Eq. (IV.21) becomes

$$M_z^I(t) = M_z^I(\infty) + (\sigma_{I(J)}/\rho_I)M_z^J(\infty)[1 - \exp(-\rho_I t)] \tag{IV.23}$$

by setting $M_z^J(\infty) = M_z^I(\infty)$ and rearranging we obtain the equation for truncated NOE:

$$\frac{M_z^I(t) - M_z^I(\infty)}{M_z^I(\infty)} = \eta_{I(J)}(t) = [\sigma_{I(J)}/\rho_I][1 - \exp(-\rho_I t)] \tag{6.17}$$

Appendix V. Simulation of NMR spectra

I. Bertini, C. Luchinat, A. Rosato

V.1. What are simulated spectra good for?

Writing or understanding a pulse sequence is a task almost every NMR spectroscopist has dealt with in his life. In principle an experiment can be theoretically analyzed in order to predict the results arising when a given set of parameters is employed. In practice, pulse sequences are often tested with little preliminary theoretical studies, and a huge amount of time can be spent to properly set experimental conditions. This is particularly true when dealing with paramagnetic compounds which, as we have already seen in Chapters 7 and 9, often require unusual settings. However, NMR time is precious and one would like to cut down the amount required for testing experiments. Simulations can help a lot in this. Setting up the simulation of an experiment, if a library of simulations of the effects of various pulses is available, reduces merely to glueing together the different pieces. Acquiring a simulated spectrum generally takes much shorter than acquiring a real spectrum, and, in any case, CPU time is usually less precious than NMR time. Furthermore, one can play with the sequence and try to improve it or to understand it better, just trying to change the pulses, to skip some part of the sequence, etc. Let us think of an experiment in which shaped pulses are used; changing one (or more) of them into a hard pulse will help understanding its function. To a researcher who is familiar with NMR, the results of such changes may be obvious; nevertheless, the possibility of having a look at what really happens (or should happen), without wasting energy, is something one should appreciate. Of course, owing to the fact that up to now simulations can be run only on ideal, small systems, it is not possible to explore all the features of an experiment. A pulse sequence needs real testing as well. A simple example can be that of a too long high power decoupling, which would not have any particular consequence in a simulation, but would destroy the sample in real life

Even well-known experiments can benefit from a clever use of simulations. From a 2D experiment to the most fancy *n*D experiment, there are always parameters to be adjusted to achieve the best results. Again, this could be (and in some cases has been) done through a detailed theoretical analysis, but instead it is often done by hand. This procedure is time consuming, and one is never sure of working with the best set of parameters. The right set of parameters for a certain system can be evaluated through simulations.

Another possible use of simulations is the inspection of the shape of peaks. Sometimes, owing to some peculiarity either of the system studied or of the experiment, the spectrum detected shows some odd patterns. For instance, superimposition of pure absorption or pure dispersion lineshapes may result in an unusual aspect of a peak.

V.2. Product operators[1]

The evolution of magnetization during NMR experiments can be followed by means of the so-called product operators formalism. This approach has the advantage of being simple, and of being pictorially representable.

The basic idea of this approach is that of representing the magnetization of one spin through a combination of spin angular momentum operators. For instance, magnetization of a spin I can be represented through a linear combination of the three operators I_x, I_y, I_z. In the presence of an external magnetic field, the nuclear spin will be aligned along the direction of the field, say z; its magnetization is then represented by (is proportional to) I_z. A generic α degrees pulse applied along one of the in-plane axes will produce a rotation of the magnetization vector around that axis of α degrees. This means that after a 90° pulse applied along the y axis, magnetization will be along the x axis (Fig. V.1), and therefore will be represented by I_x.[2]

If the nuclear spin has a Larmor frequency ω, then its time evolution under the effect of chemical shift is given by the following rules:

$$\begin{aligned} I_z &\rightarrow I_z \\ I_x &\rightarrow I_x \cos \omega t + I_y \sin \omega t \\ I_y &\rightarrow I_y \cos \omega t - I_x \sin \omega t \end{aligned} \qquad \text{(V.1)}$$

This kind of representation for a single nuclear spin is absolutely equivalent to the classic vector model.

Things get a little bit more complicated when one has to deal with a two spin (I, K) system. In this case, the spin system is described by a combination of the following spin operators:

$$\begin{aligned} &I_x, I_y, I_z \\ &K_x, K_y, K_z \\ &I_xK_x, I_yK_x, I_zK_x, I_xK_y, I_yK_y, I_zK_y, I_xK_z, I_yK_z, I_zK_z \end{aligned}$$

Notice that the latter nine operators are formed by all the possible products (hence the name of the formalism), two at a time, of the three spin angular momentum operators of spin I and the three spin angular momentum operators of spin K. Vector representations of all these operators are shown in Fig. V.1.

In the presence of an external magnetic field, the two nuclear spins will be aligned along z and their magnetization will be represented by the operators I_z and K_z. If I and K are two spins of the same nuclear species, after a non-selective pulse applied along the y axis, their magnetization will be represented by I_x and K_x respectively. Evolution under the effect of chemical shift is still given by Eqs. (V.1). Spin I will

[1] This appendix will deal only with spin ½ nuclei. However, extensions of this approach have been developed for other nuclear spins.

[2] The convention used here is that a pulse applied along the y axis rotates spin magnetization from the z axis to the positive side of the x axis.

precess with frequency ω_I, and spin K will precess with frequency ω_K. So far, each spin behaves as it would do if the other spin were not present. However, if the two spins are coupled, the evolution of one spin will affect the evolution of the other spin as well. Let us restrict ourselves, for the sake of simplicity, to the case of scalar

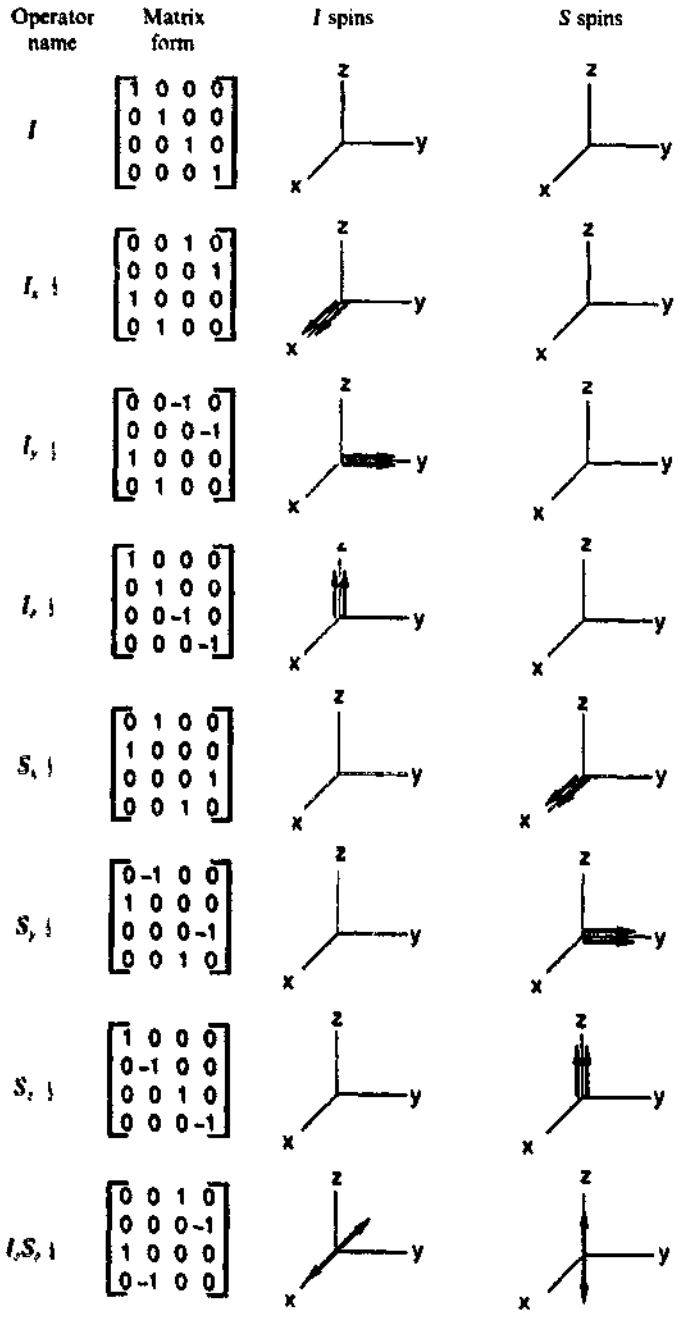

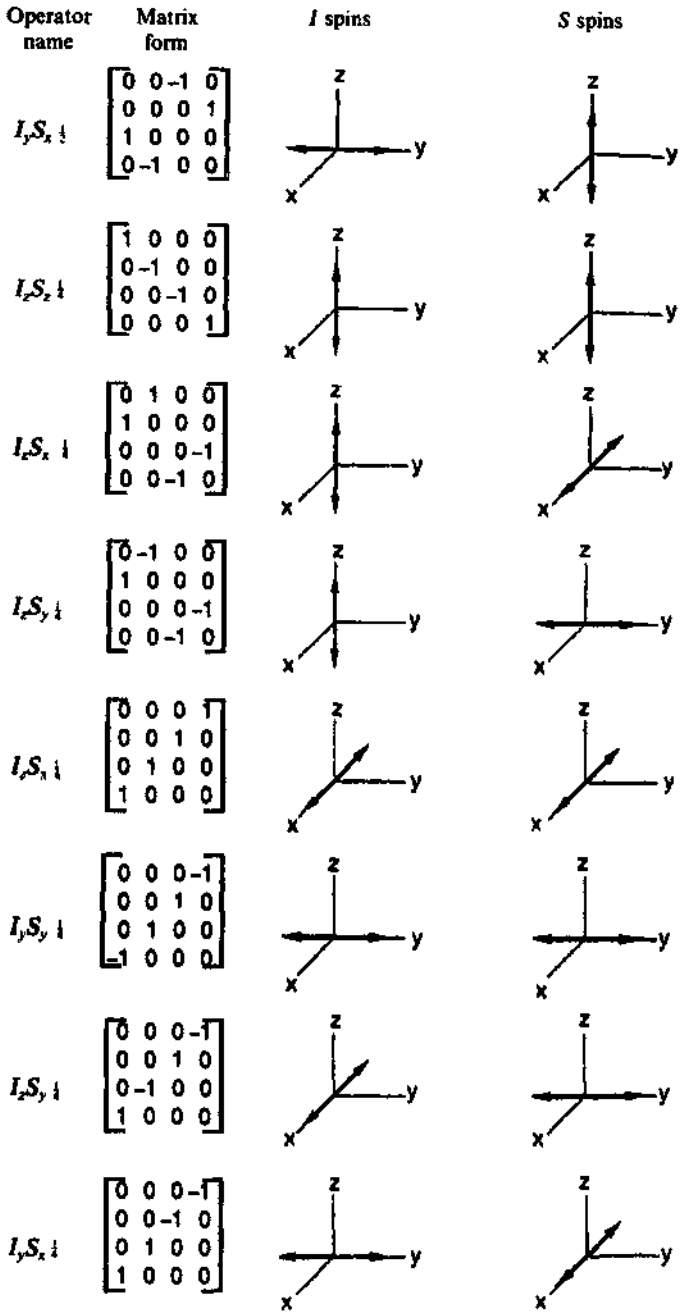

Fig. V.1. Product operators for a two-spin system. The density matrix form is shown along with the vector representation (from Ref. [5], p. 8).

coupling in solution, the coupling constant between I and K being J. The effect of scalar coupling on the time evolution of one spin (say spin I) can be computed from the following equations:

$$
\begin{aligned}
&I_z \rightarrow I_z \\
&I_x \rightarrow I_x \cos \pi Jt + 2I_yK_z \sin \pi Jt \\
&I_y \rightarrow I_y \cos \pi Jt - 2I_xK_z \sin \pi Jt \\
&2I_yK_z \rightarrow 2I_yK_z \cos \pi Jt - I_x \sin \pi Jt \\
&2I_xK_z \rightarrow 2I_xK_z \cos \pi Jt + I_y \sin \pi Jt
\end{aligned}
\qquad \text{(V.2)}
$$

The same holds for spin K; the effect is still described by Eqs. (V.2), in which I and K are swapped.

The effects of chemical shift and scalar coupling on the time evolution of one spin can be accounted for independently, regardless of the order (the two effects are said to commute). For example:

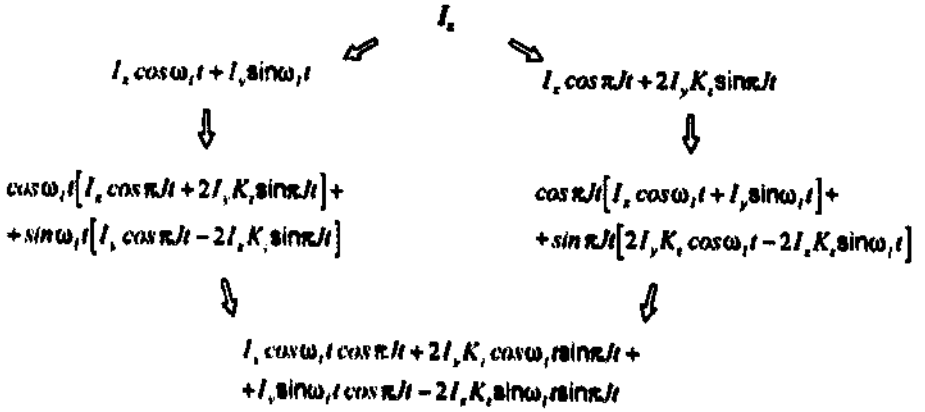

In other words, in a term which is the product of two operators, each operator evolves under the effect of chemical shift and scalar coupling independently. A further example is

$$I_xK_y \xrightarrow{\omega_I,\omega_K}$$

$$
\begin{aligned}
&I_x \cos \omega_I t[K_y \cos \omega_K t - K_x \sin \omega_K t] + I_x \sin \omega_I t[K_y \cos \omega_K t - K_x \sin \omega_K t] \\
&\quad = I_xK_y \cos \omega_I t \cos \omega_K t - I_xK_x \cos \omega_I t \sin \omega_K t + I_xK_y \sin \omega_I t \cos \omega_K t \\
&\qquad - I_xK_x \sin \omega_I t \sin \omega_K t
\end{aligned}
$$

Unfortunately, there is an exception: a term which is product of two transverse operators does not evolve under scalar coupling between the two spins. That is, scalar coupling between I and K does not affect terms like I_xK_x, I_xK_y, etc. Anyway, one should keep in mind that such terms do evolve under the effect of scalar coupling to a third nucleus. As an example, suppose that spin I is coupled to spin S with a

constant J_{IS}:

$$I_xK_x \xrightarrow{\pi J_{IS}t} I_xK_x \cos \pi J_{IS}t + 2I_yK_xS_z \sin \pi J_{IS}t$$

Note that the operator K_x just acts as a multiplicative constant.

In products of two operators, each one evolves independently also under the effect of pulses. For instance:

$$I_zK_z \xrightarrow{90^\circ_y} I_xK_x$$

$$I_xK_y \xrightarrow{90^\circ_y} -I_zK_y$$

As can be understood by looking at Fig. V.1, only single spin operators correspond to directly detectable magnetization. So, in common NMR experiments, only terms like I_x, I_y, K_x, K_y correspond to an observable, whereas all other terms (I_xK_x, I_xK_y, I_yK_z, etc.) are not directly observable.

By means of the few basic ideas exposed so far it is possible to follow a COSY experiment. Say the two coupled nuclei are I and K, the coupling constant between the two being J. We can follow the evolution of one spin: the evolution of the other can be easily obtained by swapping the I and K operators. After the first 90°_y pulse, z magnetization is converted into x magnetization. Then, evolution during t_1 follows

$$I_x \rightarrow I_x \cos \omega_I t_1 \cos \pi Jt_1 + 2I_yK_z \cos \omega_I t_1 \sin \pi Jt_1 + I_y \sin \omega_I t_1 \cos \pi Jt_1$$
$$- 2I_xK_z \sin \omega_I t_1 \sin \pi Jt_1$$

After the second 90° pulse is applied along the x axis, the system is transformed into

$$I_x \cos \omega_I t_1 \cos \pi Jt_1 - 2I_zK_y \cos \omega_I t_1 \sin \pi Jt_1 + I_z \sin \omega_I t_1 \cos \pi Jt_1$$
$$+ 2I_xK_y \sin \omega_I t_1 \sin \pi Jt_1$$

At this point, signal detection occurs. As I_z and $2I_xK_y$ do not yield observable magnetization, the third and fourth terms are of no further interest and will be dropped. During t_2, the evolution of the first two terms is as follows (only relevant terms are shown):

$$I_x \cos \omega_I t_1 \cos \pi Jt_1 \rightarrow I_x \cos \omega_I t_1 \cos \pi Jt_1 \cos \omega_I t_2 \cos \pi Jt_2$$
$$+ I_y \cos \omega_I t_1 \cos \pi Jt_1 \sin \omega_I t_2 \cos \pi Jt_2 + \ldots$$
$$-2I_zK_y \cos \omega_I t_1 \sin \pi Jt_1 \rightarrow K_x \cos \omega_I t_1 \sin \pi Jt_1 \cos \omega_K t_2 \sin \pi Jt_2$$
$$+ K_y \cos \omega_I t_1 \sin \pi Jt_1 \sin \omega_K t_2 \sin \pi Jt_2 + \ldots$$

The terms in the first row give rise to a peak at frequency ω_I in the first dimension and ω_I in the second dimension: that is, they give rise to the diagonal peak of spin I. The peak arising from the terms in the second row has frequency ω_K in the first

dimension and ω_I in the second dimension, thus yielding a cross-peak between I and K. If one carries out the same calculation starting from K, its diagonal peak and the cross-peak between I and K at $(\omega_I; \omega_K)$ are obtained.

Product operators can thus be used to predict the behavior of an NMR experiment. The calculations are relatively simple to perform. Computer programs are available that also take into account the effects of phase-cycling to select the desired terms and reject unwanted ones. A drawback of the product operators approach is that, in its simplest version, it does not take into account the effect of relaxation. This is a must when dealing with paramagnetic substances. Exponential decay terms can be introduced to multiply each term and take relaxation into account. The method then becomes more cumbersome, and the effect of relaxation is introduced in a phenomenological way. A better approach is that of using the concept of Redfield density matrix.

V.3. Density matrix

In general, a spin system can be described by a function $|\Psi\rangle$, which in turn can be written as a summation of the eigenfunctions of the nuclear Zeeman Hamiltonian, each multiplied by an appropriate coefficient

$$|\Psi\rangle = \sum_\gamma c_\gamma |\gamma\rangle \tag{V.3}$$

For a two-spin $\frac{1}{2}$ system we have[3]

$$|\Psi\rangle = c_{\alpha\alpha}|\alpha\alpha\rangle + c_{\alpha\beta}|\alpha\beta\rangle + c_{\beta\alpha}|\beta\alpha\rangle + c_{\beta\beta}|\beta\beta\rangle \tag{V.4}$$

Since the system passes from one Zeeman eigenstate to another with time, the function $|\Psi\rangle$ will in general be a function of time, whereas the eigenfunctions of the nuclear Zeeman Hamiltonian are not. Then, the coefficients c_γ must be time dependent. Eq. (V.3) can be rewritten as follows:

$$|\Psi(t)\rangle = \sum_\gamma c_\gamma(t)|\gamma\rangle \tag{V.5}$$

The evolution of the system, that is the evolution of $|\Psi(t)\rangle$, is accounted for by the coefficients $c_\gamma(t)$. For the sake of simplicity, in the following $|\Psi(t)\rangle$ will be indicated just by $|\Psi\rangle$, still being time dependent.

The expectation value of an operator $\hat{A}$ is given by

$$\langle A\rangle = \langle\Psi|\hat{A}|\Psi\rangle \tag{V.6}$$

When dealing with a macroscopic sample, the value observed will be the ensemble average of the expectation values for all individual spin systems.

$$\overline{\langle A\rangle} = \overline{\langle\Psi|\hat{A}|\Psi\rangle} \tag{V.7}$$

[3] Throughout this appendix, nuclear spin states will be indicated as $|\alpha\rangle$ and $|\beta\rangle$ instead of $|+\rangle$ and $|-\rangle$ as elsewhere in the book.

Recalling Eq. (V.5), we obtain

$$\overline{\langle A\rangle} = \sum_{\gamma}\sum_{\lambda} \overline{c_{\gamma}^{*}(t)c_{\lambda}(t)}\langle\gamma|\hat{A}|\lambda\rangle = \sum_{\gamma}\sum_{\lambda} \overline{c_{\gamma}^{*}(t)c_{\lambda}(t)}A_{\gamma\lambda} \tag{V.8}$$

The elements $A_{\gamma\lambda}$ are constant for a given spin system and constitute the matrix representation of $\hat{A}$ in the eigenbasis chosen.

The elements of the density matrix are defined as

$$\sigma_{\lambda\gamma} = \overline{c_{\gamma}^{*}(t)c_{\lambda}(t)} \tag{V.9}$$

Eq. (V.8) then becomes

$$\overline{\langle A\rangle} = \sum_{\gamma}\sum_{\lambda} \sigma_{\lambda\gamma}A_{\gamma\lambda} \tag{V.10}$$

which corresponds to summing all the diagonal elements of the matrix resulting from the product of A and σ. Eq. (V.10) can thus be rewritten

$$\overline{\langle A\rangle} = \mathrm{Tr}\{A\sigma\} \tag{V.11}$$

where Tr stands for trace of the matrix $A\sigma$.

Let us now have a look at an example. A single spin $\frac{1}{2}$ system is described by a 2×2 matrix:

$$\sigma = \begin{array}{c|cc} & |\alpha\rangle & |\beta\rangle \\ \hline \langle\alpha| & \mathrm{Pop}^{\alpha} & \mathrm{SQ} \\ \langle\beta| & \mathrm{SQ} & \mathrm{Pop}^{\beta} \end{array}$$

The two diagonal elements describe the population of the states α and β. Off-diagonal elements are related to single quantum transitions (SQ).

For a two-spin $\frac{1}{2}$ system (Fig. V.2) we have a 4×4 matrix:

$$\sigma = \begin{array}{c|cccc} & |\alpha\alpha\rangle & |\alpha\beta\rangle & |\beta\alpha\rangle & |\beta\beta\rangle \\ \hline \langle\alpha\alpha| & \mathrm{Pop}^{\alpha\alpha} & \mathrm{SQ}^{K} & \mathrm{SQ}^{I} & \mathrm{DQ} \\ \langle\alpha\beta| & \mathrm{SQ}^{K} & \mathrm{Pop}^{\alpha\beta} & \mathrm{ZQ} & \mathrm{SQ}^{I} \\ \langle\beta\alpha| & \mathrm{SQ}^{I} & \mathrm{ZQ} & \mathrm{Pop}^{\beta\alpha} & \mathrm{SQ}^{K} \\ \langle\beta\beta| & \mathrm{DQ} & \mathrm{SQ}^{I} & \mathrm{SQ}^{K} & \mathrm{Pop}^{\beta\beta} \end{array}$$

Diagonal elements describe the population of the four states. Off-diagonal elements are related to terms that connect different states (that is transitions). Terms which describe the flipping of one spin (e.g. $\alpha\alpha \nrightarrow \alpha\beta$) are related to single quantum transitions (SQ); terms which describe the flipping of both spins in opposite directions (e.g. $\beta\alpha \rightarrow \alpha\beta$) are related to zero quantum transitions (ZQ); terms which describe the flipping of both spins in the same direction (e.g. $\alpha\alpha \rightarrow \beta\beta$) are related to double quantum transitions (DQ).

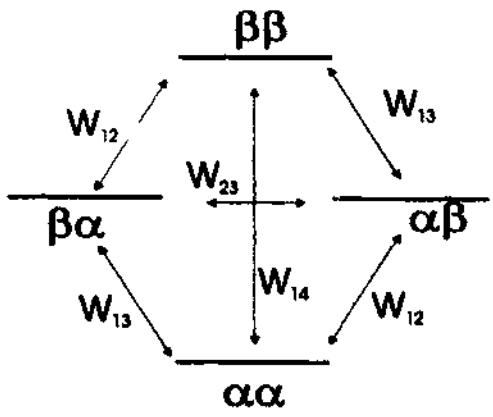

Fig. V.2. Energy levels and transition probabilities for a two-spin system.

When the system is at thermal equilibrium, the relative population of levels is given by the Boltzmann distribution. For a two homonuclear spin system we have (neglecting small energy differences due to chemical shifts and scalar coupling)

$$\frac{\mathrm{Pop}^{\alpha\alpha}}{\mathrm{Pop}^{\alpha\beta}} \approx 1 + \frac{h\nu}{kT} = 1 + p$$

$$\frac{\mathrm{Pop}^{\alpha\beta}}{\mathrm{Pop}^{\alpha\beta}} = 1$$

$$\frac{\mathrm{Pop}^{\beta\alpha}}{\mathrm{Pop}^{\alpha\beta}} = 1$$

$$\frac{\mathrm{Pop}^{\beta\beta}}{\mathrm{Pop}^{\alpha\beta}} \approx 1 - \frac{h\nu}{kT} = 1 - p$$

where h is Planck's constant, ν is the frequency of the proton, k is Boltzmann's constant, and T is the absolute temperature. The density matrix at thermal equilibrium is then

$$\sigma_{eq} = \frac{1}{4}\begin{bmatrix} 1 & 0 & 0 & 0 \\ 0 & 1 & 0 & 0 \\ 0 & 0 & 1 & 0 \\ 0 & 0 & 0 & 1 \end{bmatrix} + \frac{p}{4}\begin{bmatrix} 1 & 0 & 0 & 0 \\ 0 & 0 & 0 & 0 \\ 0 & 0 & 0 & 0 \\ 0 & 0 & 0 & -1 \end{bmatrix} \tag{V.12}$$

The first matrix, which is the identity matrix, is not affected by any phenomenon of interest in NMR spectroscopy and therefore can be neglected.

The density matrix allows one to fully describe the evolution of the system through pulses, chemical shift and scalar coupling.

A pulse with flip angle α applied along the x-axis of the rotating frame transforms the density matrix σ into another matrix σ'. The relationship between the two is

$$\sigma' = \mathbf{R}_y^{-1}(\alpha)\sigma\mathbf{R}_y(\alpha) = \mathbf{R}_y^{\dagger}\sigma\mathbf{R}_y(\alpha) \tag{V.13}$$

where $\mathbf{R}_y(\alpha)$ is a rotation matrix and $\mathbf{R}_y^{\dagger}(\alpha)$ is its transpose conjugate. For a 90°_y rotation of a two-spin system

$$\mathbf{R}_y = \frac{1}{2}\begin{bmatrix} 1 & 1 & 1 & 1 \\ -1 & 1 & -1 & 1 \\ -1 & -1 & 1 & 1 \\ 1 & -1 & -1 & 1 \end{bmatrix} \tag{V.14}$$

Therefore, the result of the application of a 90°_y pulse to a two-spin system whose equilibrium density matrix is given by Eq. (V.12) is

$$\sigma_1 = \frac{1}{2}\begin{bmatrix} 1 & -1 & -1 & 1 \\ 1 & 1 & -1 & -1 \\ 1 & -1 & 1 & -1 \\ 1 & 1 & 1 & 1 \end{bmatrix} \frac{p}{4}\begin{bmatrix} 1 & 0 & 0 & 0 \\ 0 & 0 & 0 & 0 \\ 0 & 0 & 0 & 0 \\ 0 & 0 & 0 & -1 \end{bmatrix} \frac{1}{2}\begin{bmatrix} 1 & 1 & 1 & 1 \\ -1 & 1 & -1 & 1 \\ -1 & -1 & 1 & 1 \\ 1 & -1 & -1 & 1 \end{bmatrix}$$

$$= \frac{p}{8}\begin{bmatrix} 0 & 1 & 1 & 0 \\ 1 & 0 & 0 & 1 \\ 1 & 0 & 0 & 1 \\ 0 & 1 & 1 & 0 \end{bmatrix} \tag{V.15}$$

Analogous matrices can be written for pulses along different axes. The time evolution of the density matrix under the effect of a time independent Hamiltonian, when the scalar coupling is weak, is given by

$$\sigma_{\gamma\lambda}(t) = \exp\left[-\frac{i}{\hbar}(E_\gamma - E_\lambda)t\right]\sigma_{\gamma\lambda}(0) \tag{V.16}$$

E_γ and E_λ being the energies of the states $|\gamma\rangle$ and $|\lambda\rangle$ respectively.

Relaxation can be simply included as an exponential decay of the off-diagonal elements of the matrix. Suitable equations to derive relaxation rates for the various matrix elements are available in the literature. Therefore, the time evolution due to chemical shift, scalar coupling and transverse relaxation transforms σ_1 into

$$\sigma_2 = \frac{p}{8}\begin{bmatrix} 0 & \exp[-i(\omega_K + \pi J)t]\exp(-R_{2K}t) & \exp[-i(\omega_I + \pi J)t]\exp(-R_{2I}t) & 0 \\ \exp[i(\omega_K + \pi J)t]\exp(-R_{2K}t) & 0 & 0 & \exp[i(\omega_I - \pi J)t]\exp(-R_{2I}t) \\ \exp[i(\omega_I + \pi J)t]\exp(-R_{2I}t) & 0 & 0 & \exp[-i(\omega_K - \pi J)t]\exp(-R_{2K}t) \\ 0 & \exp[-i(\omega_I + \pi J)t]\exp(-R_{2I}t) & \exp[i(\omega_K - \pi J)t]\exp(-R_{2K}t) & 0 \end{bmatrix} \tag{V.17}$$

Note that longitudinal relaxation has been neglected.

The intensity of magnetization detected at a certain time M is given (if quadrature detection is performed) by the sum of expectation values (ensemble averaged) of the operator $\hat{I}_x + i\hat{I}_y = \hat{I}_+$ for all I spins (and the same for the K spins) times $N_0\gamma\hbar$, that is

$$M = \sum_{I=1}^{N} N_0\gamma\hbar\overline{\langle \hat{I}_x + i\hat{I}_y \rangle} \tag{V.18}$$

where N_0 is the number of spins per unit volume; γ is the magnetogyric ratio of the spins. The matrix representation of $\mathbf{I}_+$ is

$$\mathbf{I}_+ = \begin{bmatrix} 0 & 1 & 1 & 0 \\ 0 & 0 & 0 & 1 \\ 0 & 0 & 0 & 1 \\ 0 & 0 & 0 & 0 \end{bmatrix} \tag{V.19}$$

Therefore, recalling Eq. (V.11), we obtain

$$\begin{aligned} M = N_0\gamma\hbar\frac{p}{8}\{&\exp[-i(\omega_K + \pi J)t]\exp(-R_{2K}t) \\ &+ \exp[-i(\omega_K - \pi J)t]\exp(-R_{2K}t) \\ &+ \exp[-i(\omega_I + \pi J)t]\exp(-R_{2I}t) \\ &+ \exp(-i(\omega_I - \pi J)t]\exp(-R_{2I}t)\} \end{aligned} \tag{V.20}$$

The intensity of the magnetization has to be evaluated at different, equally-spaced values of t, in order to have a simulated FID, which can be then Fourier transformed. With these tools it is possible to simulate a spectrum, including relaxation.

A few examples should clarify the concepts exposed so far. As a first example of a 2D experiment, let us take the COSY experiment. Immediately before the mixing pulse, the system will be described by the density matrix σ_2 (Eq. (V.17)). Then a second 90° pulse is applied, for example along the y axis, which transforms σ_2 according to Eq. (V.13).

$$\sigma_2(t_1) \xrightarrow{90^\circ_y} \sigma_3(t_1)$$

Then, time evolution has to be evaluated during t_2.

$$\sigma_3(t_1) \xrightarrow{\text{Time evolution}} \sigma_4(t_1; t_2)$$

And finally the intensity of magnetization detected can be computed through Eqs. (V.11) and (V.18).

$$M(t_1; t_2) = N_0\gamma\hbar\,\mathrm{Tr}\{\mathbf{I}_+\sigma(t_1; t_2)\}$$

To collect an ensemble of FIDs we must, just like in a real experiment, fix t_1 at a

certain value and then evaluate M as a function of t_2. In this way an FID is 'recorded', which can be written to a file; then t_1 is (regularly) increased and another FID is calculated. The whole procedure is repeated until the desired number of experiments is recorded. When the simulation is over, one is left with a file containing all the FIDs, which can be dealt with just like a real experiment. Note that, having neglected longitudinal relaxation during t_1, some artifacts will be missing in the resulting spectrum.

Let us now move to a more complex example, that is the NOESY experiment. Longitudinal cross-relaxation cannot be accounted for by the simple treatment we have used in the previous example. A deeper analysis is required in order to produce a simulation of a NOESY spectrum. The time dependence of populations is given by

$$\frac{\mathrm{d}}{\mathrm{d}t}\begin{bmatrix} P^{\alpha\alpha}(t) \\ P^{\alpha\beta}(t) \\ P^{\beta\alpha}(t) \\ P^{\beta\beta}(t) \end{bmatrix} = \begin{bmatrix} W_{11} & W_{12} & W_{13} & W_{14} \\ W_{21} & W_{22} & W_{23} & W_{24} \\ W_{31} & W_{32} & W_{33} & W_{34} \\ W_{41} & W_{42} & W_{43} & W_{44} \end{bmatrix} \begin{bmatrix} P^{\alpha\alpha}(t) - P^{\alpha\alpha}_{\mathrm{eq}} \\ P^{\alpha\beta}(t) - P^{\alpha\beta}_{\mathrm{eq}} \\ P^{\beta\alpha}(t) - P^{\beta\alpha}_{\mathrm{eq}} \\ P^{\beta\beta}(t) - P^{\beta\beta}_{\mathrm{eq}} \end{bmatrix} \tag{V.21}$$

where the Ps have the known meaning (see above), and the Ws are transition probabilities (Fig. V.2). The approach to the calculation of the Ws is described in the literature. The matrix $\boldsymbol{W}$ is symmetrical, that is $W_{mn} = W_{nm}$. To simulate a NOESY spectrum, longitudinal relaxation needs to be computed during the mixing time. The evolution of the system up to the end of t_1 is again described by Eq. (V.17); then a 90° pulse is applied which transforms σ_2 into σ_3. Now the time evolution of the system is to be evaluated through Eq. (V.21). The simplest way to do that is to divide t_m into the sum of many short $\mathrm{d}t$ and to assume that each difference $P(t) - P_{\mathrm{eq}}$ is constant over each $\mathrm{d}t$. In this way we obtain

$$\begin{bmatrix} P^{\alpha\alpha}(t + j\,\mathrm{d}t) \\ P^{\alpha\beta}(t + j\,\mathrm{d}t) \\ P^{\beta\alpha}(t + j\,\mathrm{d}t) \\ P^{\beta\beta}(t + j\,\mathrm{d}t) \end{bmatrix} = \begin{bmatrix} W_{11} & W_{12} & W_{13} & W_{14} \\ W_{21} & W_{22} & W_{23} & W_{24} \\ W_{31} & W_{32} & W_{33} & W_{34} \\ W_{41} & W_{42} & W_{43} & W_{44} \end{bmatrix} \begin{bmatrix} P^{\alpha\alpha}(t + (j-1)\,\mathrm{d}t) - P^{\alpha\alpha}_{\mathrm{eq}} \\ P^{\alpha\beta}(t + (j-1)\,\mathrm{d}t) - P^{\alpha\beta}_{\mathrm{eq}} \\ P^{\beta\alpha}(t + (j-1)\,\mathrm{d}t) - P^{\beta\alpha}_{\mathrm{eq}} \\ P^{\beta\beta}(t + (j-1)\,\mathrm{d}t) - P^{\beta\beta}_{\mathrm{eq}} \end{bmatrix} * \mathrm{d}t$$

$$j = 1, 2, \ldots, n; \quad n \times \mathrm{d}t = t_m$$

The above expression is evaluated iteratively until $j = n$, yielding the final value of the four $P(t_1 + t_m)$ values. Note that neglecting longitudinal relaxation during t_1 introduces only a minor error. This accounts for evolution of diagonal elements of the density matrix. The evolution of off-diagonal elements will be dealt with in the usual way. Finally, application of the third 90° pulse, evolution during t_2, and acquisition are straightforward operations.

A final comment is due to phase cycling. Its effect can be simulated by varying the phases of different pulses and summing up the resulting FIDs before writing them to disk, just like in real life.

One must keep in mind that including relaxation in the way we described above

is also an approximation. However, the experimental behavior is often close enough to what has been just described. Our last example shows a case in which the approximation of an exponential recovery cannot be used. Subtle effects cannot be investigated with the approach we have used. A more cumbersome formalism, the superoperator formalism, is required to quantitatively evaluate and simulate such effects. Within this limit, density matrix approach still proves useful.

V.4. Final remarks

The use of simulations can help a researcher a lot in his work. This is particularly true when dealing with paramagnetic systems. The effect of the shortening of nuclear relaxations rates caused by paramagnetism can be predicted, and different conditions and experiments can be tested. This allows one to maximize the amount of information detectable through NMR.

The results of simulations performed on paramagnetic systems have proved useful in many situations, as shown in the literature.

The sources of some Fortran programs for the simulation of the most common experiments are available through anonymous ftp at the site: risc2.lrm.fi.cnr.it, in the directory /pub/nmr-sim. Information can be obtained from Antonio Rosato, e-mail: Antonio@risc1.lrm.fi.cnr.it.

V.5. Bibliography

[1] A. Bax, Two Dimensional Nuclear Magnetic Resonance in Liquids, Reidel, Dordrecht, 1982.
[2] O.W. Sorensen and R.R. Ernst, J. Magn. Reson., 51 (1983) 477.
[3] N. Chandrakumar, J. Magn. Reson., 60 (1984) 28.
[4] R.R. Ernst, G. Bodenhausen, and A. Wokaun, Principles of Nuclear Magnetic Resonance in One and Two Dimensions, Oxford University Press, London, 1987.
[5] J. Shriver, Concepts Magn. Reson., 4 (1992) 1–34.

Appendix VI. Reference tables

Physical and mathematical constants

Quantity	Symbol	Value	
		SI	CGS emu
Physical constants			
Permeability of vacuum	μ_0	$4\pi \times 10^{-7}$ kg m s^{-2} A^{-2}	1
Speed of light in vacuo	c	2.9979×10^{8} m s^{-1}	2.9979×10^{10} cm s^{-1}
Elementary charge (absolute value of the electron charge)	e	1.6022×10^{-19} A s	1.6022×10^{-20} abcoulombs
Planck constant	h	6.6262×10^{-34} J s	6.6262×10^{-27} erg s
	$\hbar = h/2\pi$	1.0546×10^{-34} J s rad^{-1}	1.0546×10^{-27} erg s rad^{-1}
Avogadro constant	N_A	6.0220×10^{23} mol^{-1}	
Electron rest mass	m_e	0.9110×10^{-30} kg	0.9110×10^{-27} g
Proton rest mass	m_p	1.6726×10^{-27} kg	1.6726×10^{-24} g
Free-spin electron g factor	g_e	2.0023	
Electron Bohr magneton	μ_B	9.2741×10^{-24} J T^{-1}	9.2741×10^{-21} erg G^{-1}
Nuclear Bohr magneton	μ_B	5.0508×10^{-27} J T^{-1}	5.0508×10^{-24} erg G^{-1}
Free-electron magnetic moment	$\mu_e = \frac{g_e \mu_B}{2}$	9.2848×10^{-24} J T^{-1}	9.2848×10^{-21} erg G^{-1}
Proton magnetic moment	$\mu_p = \frac{g_p \mu_N}{2}$	1.4106×10^{-26} J T^{-1}	1.4106×10^{-23} erg G^{-1}
Electron-to-proton magnetic moments ratio	μ_e/μ_p	658.21	
Free-electron magnetogyric ratio	γ_e	1.7608×10^{11} rad s^{-1} T^{-1}	1.7608×10^{7} rad s^{-1} G^{-1}
Proton magnetogyric ratio	γ_p	2.6752×10^{8} rad s^{-1} T^{-1}	2.6752×10^{4} rad s^{-1} G^{-1}
Boltzmann constant	k	1.3807×10^{-23} J K^{-1}	1.3807×10^{-16} erg K^{-1}
Hyperfine coupling constant of the hydrogen atom	$(a/h)_H$	1.4204×10^{9} Hz	
	$(a/\hbar)_H$	8.9247×10^{9} rad s^{-1}	
Mathematical constants			
	e	2.7183	
	π	3.1416	

Conversion factors

Quantity	To convert from	To	Multiply by
Length	angstroms (Å)	meters (m)	1×10^{-10}
Pressure	atmospheres (atm)	pascals (Pa) ($kg\ m^{-1}\ s^{-2}$)	1.01325×10^{5}
Mass	atomic mass unit (amu)	kilograms (kg)	1.6606×10^{-27}
Energy	calories (cal)	joules (J)	4.1840
	electron volts (eV)	joules (J)	1.6022×10^{-19}
	kilowatt-hours (kWh)	joules (J)	3.6×10^{6}
Viscosity	centipoises	$kg\ m^{-1}\ s^{-1}$	1×10^{-3}
Angles	degrees (deg)	radians (rad)	0.017453
Volume	litres (l)	cubic meters (m^3)	1×10^{-3}
Frequency	radians/seconds (rad s^{-1})	cycles/seconds (cps) (Hz)	0.15915
	wavenumber (cm^{-1})	energy (J)	1.9865×10^{-23}
		frequency (s^{-1}) (Hz)	2.9979×10^{10}
		frequency (rad s^{-1})	1.8837×10^{11}
	frequency (s^{-1}) (Hz)	energy (J)	6.6262×10^{-34}
	temperature (K)	energy (J)	1.3807×10^{-23}
		wavenumber (cm^{-1})	0.69467

Some physical quantities and their SI units

Electric charge (quantity of electricity)	Q	C	A s
Electric current	I	A	A
Electric potential	V	V	$kg\ m^2\ s^{-3}\ A^{-1}$ ($= J\ A^{-1}\ s^{-1}$)
Energy	E	J	$kg\ m^2\ s^{-2}$
Frequency	ν	Hz	s^{-1}
Frequency (angular velocity)	ω	rad s^{-1}	rad s^{-1}
Magnetic field strength	H	A m^{-1}	A m^{-1}
Magnetic induction (flux density)	B	T	$kg\ A^{-1}\ s^{-2}$
Magnetic moment	μ	J T^{-1}	$A\ m^2$
Magnetic susceptibility	χ	m^3	m^3
Magnetization	M	J $T^{-1}\ m^{-3}$	A m^{-1}
Magnetogyric ratio	Γ	rad $s^{-1}\ T^{-1}$	rad A s kg^{-1}
Molar magnetic susceptibility	χ_M	$m^3\ mol^{-1}$	$m^3\ mol^{-1}$
Power	P	W	$kg\ m^2\ s^{-3}$ ($= J\ s^{-1}$)
Viscosity (dynamic)	η	$kg\ m^{-1}\ s^{-1}$	$kg\ m^{-1}\ s^{-1}$